Journal of Physics: Conference Series

A Numerical Investigation of the Friction Contact of an Unfilled Styrene Butadiene Rubber by a Blade Sliding Indentation

To cite this article: B. Setiyana *et al* 2018 *J. Phys.: Conf. Ser.* **1090** 012078

IOP Conf. Series: Journal of Physics: Conf. Series **1090** (2018) 012078 doi:10.1088/1742-6596/1090/1/012078

A Numerical Investigation of the Friction Contact of an Unfilled Styrene Butadiene Rubber by a Blade Sliding Indentation

B. Setiyana[1,2,a)], M. Khafidh[2], R. Ismail[1], J.Jamari[1] and D.J. Schipper[2]

[1]Laboratory for Engineering Design and Tribology,
Department of Mechanical Engineering, University of Diponegoro,
Jl. Prof. Soedharto, Tembalang, Semarang 59275, Indonesia

[2]Laboratory for Surface Technology and Tribology,
Faculty of Engineering Technology, University of Twente,
Drienerloolaan 5, Postbus 217, 7500 AE Enschede, Dutch (Netherlands)

[a)] Corresponding author: bsetiyana@yahoo.com

Abstract. Rubber is mostly modeled as a hyperelastic material and as a consequence, large deformation occur along friction contact against a rigid counterface. In general, Coefficient of friction (COF) of a contact surface consists of two components, i.e. adhesion and deformation (hysteresis). However, it is difficult to investigate the deformation component of COF analitically on the rubber sliding. By means of a rigid blade sliding indentation technique, this paper studies the friction contact phenomena on Unfilled Styrene Butadiene Rubber (SBR-0) numerically by using a Finite Element Analysis (FEA) in plane strain mode. By a given sliding speed, the FEA simulation is carried out with the various adhesion COF and sliding depth. The presented simulation output are stress, deformation and reaction forces. Results show that the deformation COF strongly depends on the sliding displacement. Finally, the overall COF highly increases and then decreases with respect to the sliding displacement and tends to indicate stick-slip phenomena.

1. Introduction

Elastomers or rubbers are used extensively in many industries because of their wide availability and low cost. They are also used because of their excellent damping and energy absorption characteristics, flexibility, resiliency, ability to seal against moisture and variable stiffness. Rubber is a very unique material. The unique properties of rubber are such that, it can undergo large deformations under load, sustaining strains of up to 500 percent in engineering applications and its load-extension behavior is nonlinear. Proper analysis of rubber components requires special material modeling and nonlinear finite element analysis tools that are quite different than those used for metallic parts. Due to the nonlinearity behaviour and large deformation under load, rubber is mostly modeled as hyperelastic material [1]. Therefore, it is difficult to investigate the contact phenomena from the rubber friction analitically.

Most of rubber or elastomer friction has been intensively studied experimentally in sliding or abrasion contact. There were some valuable results associated with a friction contact, i.e. a coefficient of friction (COF), stick-slip occurrence, abrasive wear etc. These phenomena play an important role in investigation of a contact force and rubber life time (in case on abrasive wear). By definition, the COF consists of an adhesion component and hysteresis (deformation) component [2,3]. The adhesion component relates to interfacial friction that depends on surface contact roughness, meanwhile, the hysteresis relates to internal friction of material that strongly depends on the degree of deformation and damping value.

Rubber friction was mostly investigated experimentally as a contact between rubber and rigid rough surface [4,5]. Moreover, the friction or abrasion contact by using a single indenter was experimentally performed with a sphere, cone and blade indenter [6-10]. Along sliding contact, it obviously showed that the stick-slip phenomena occurred along friction contact and as a consequence, a periodic friction force and wear pattern were formed. The adhesion and hysteresis COF were experimentally estimated and showed that the overall COF was dominantly influenced by deformation component rather than the adhesion one [11]. A numerical investigation of the rubber friction by the blade indenter was performed to investigate the stress induced on the contact surface, meanwhile, the coefficient of friction (COF) occured was sligtly investigated [12].

By using a Finite Element Analysis (FEA), this study proposes dynamic or sliding contact in which a blade indenter tangentially slides over on the rubber surface. The material used is an Unfilled Styrene Butadiene Rubber (SBR-0) and is modeled as a hyperelastic rather than viscoelastic material because of a low damping value for unfilled rubber. The rigid blade indenter with a specified tip radius applies on the rubber surface with a constant sliding speed. The FEA output are von Mises stress on the rubber surface, deformation contour and reaction forces. The FEA simulation is carried out in various sliding depth and adhesion COF. Finally, the friction contact phenomena can be observed and the overall COF as well as the deformation COF can be developed.

2. Method

The finite element analysis of the present work was performed using a commercial finite element software package, ABAQUS 6.11 [13]. Regarding to hyperelastic model of the rubber, the material behaviour was obtained from experimental test that is required for FEA simulation and represented as Strain Energy Function (SEF) term. The SBR-0 (Unfilled Styrene Butadiene Rubber) with the Mooney-Rivlin SEF was used and the material was assumed as an incompressible material. The required data of SEF are adopted from Liang’s experiment [12] that was performed by a uniaxial tensile test up to approximately 5.5 MPa stress and 300% strain in elastic condition.

Figure 1(a) shows a schematic illustration of a straight rigid blade sliding a rubber surface. A rigid blade indenter with 0.5 mm tip radius contacts on the rubber (elastomer) surface. Boundary conditions of the indentation system are depicted schematically in this figure as well. The rubber specimen of 10 mm high, 20 mm wide and 10 mm thick was modeled in the plane strain. The constant sliding speed of 5 mm/sec, maximum horizontal sliding of 2.0 mm with some various sliding depth and adhesion COF are applied. The chosen sliding depth are 0.5, 1.0 and 2.0 mm, and the given adhesion COF are 0.0, 0.5 and 1.5.

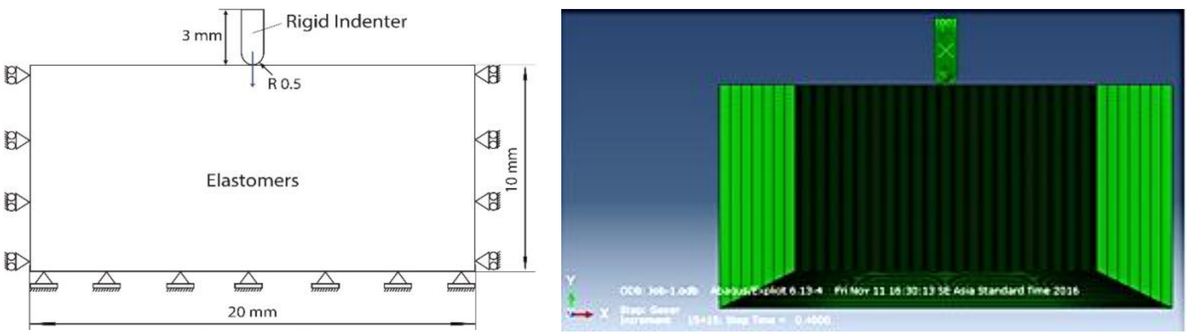

(a) (b)

Figure 1. Initial model of the rubber sliding (a) Schematic model (b) FE model

IOP Conf. Series: Journal of Physics: Conf. Series **1090** (2018) 012078 doi:10.1088/1742-6596/1090/1/012078

The FEA simulation of the blade movement is started in rest position (initial state), then to be continued in move condition (sliding state) and finally in stop condition (final state). The FEA outputs are presented in the form of stress field and deformation contour in the initial state (before sliding), the sliding state and the final state (after sliding). From these results, the reaction forces in the horizontal as well as vertical direction can be developed. By the given various adhesion COF, the deformation and overall COF can be plotted in various sliding depth with respect to the sliding displacement.

3. Results and Discussions

Fig. 2 demonstrates the FEA output of the von Mises stress field and the deformation contour surface of SBR-0 by blade sliding indentation. The FEA output with the sliding depth 0.5 mm and adhesion COF 0.5 is depicted in these figures in the initial state, the sliding state and the final state respectively. These figures show that the highest contact stresses are located below at the indenter's blade tip, especially in the initial state because it is still in static condition. It can be seen that in the sliding state, the high stress regime tends to move toward to the sliding direction. In contrast, the high stress regime moves to the opposite of the sliding direction in the final state.

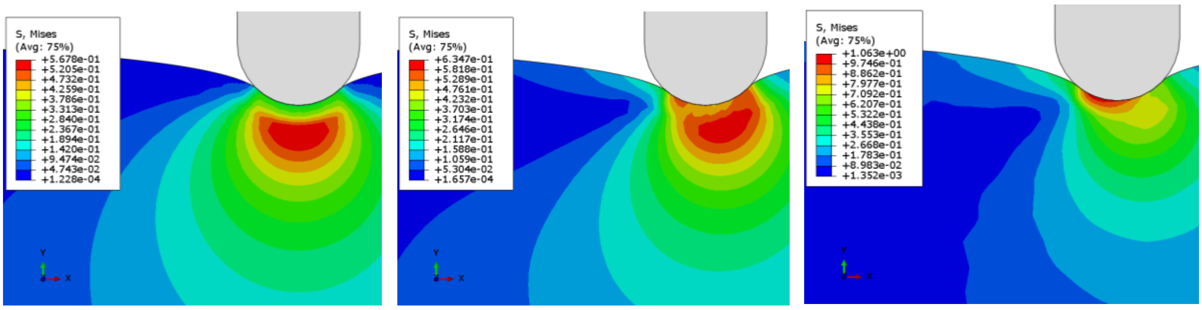

(a) (b) (c)

Figure 2. Stress field on the deformed model for sliding depth = 0.5 mm and adhesion COF = 0.5
(a) Initial state (b) Sliding state (c) Final state

The comparison of stress field on the deformed model in the sliding state is presented in Fig.3 for the various sliding depths, i.e. 0.5, 1.5 and 2.0 mm. It is clearly shown that the high stress area moves toward the sliding direction for all of the sliding state. Higher sliding depth yields to higher stress induced and located more away from the contact surface.

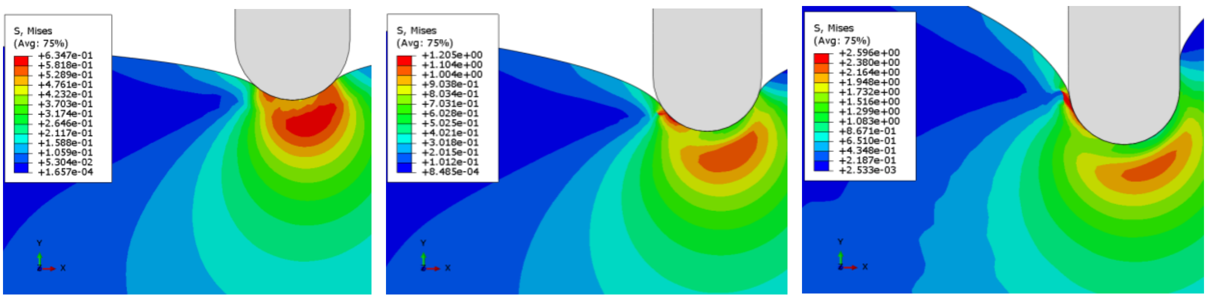

(a) (b) (c)

Figure 3. Stress field on the deformed model on sliding state for adhesion COF = 0.5
(a) Sliding depth 0.5 mm (b) Sliding depth 1.0 mm (c) Sliding depth 2.0 mm

The comparison of the stress field on the deformed model for the various adhesion COF, i.e. 0.0, 0.5 and 1.5 in the sliding state is presented in Fig.4. It is shown that the high stress area tends to move toward the sliding direction for higher adhesion COF. High adhesion COF yields to sligt increase of the maximum stress.

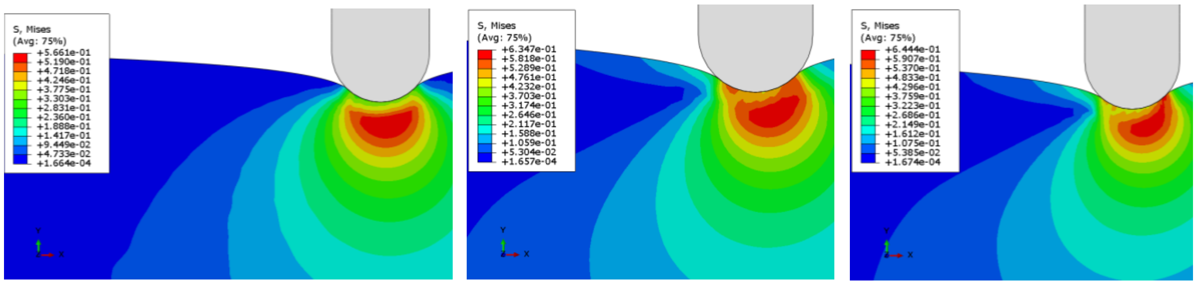

(a) (b) (c)

Figure 4. Stress distribution on the deformed model on sliding state for sliding depth = 0.5mm (a) Adhesion COF = 0 (b) Adhesion COF = 0.5 (c) Adhesion COF =1.5

The horizontal reaction forces as well as vertical reaction forces are depicted in Fig.5 and Fig.6 respectively. It can be clearly seen that horizontal reaction forces increase with respect to the sliding depth and adhesion COF. However, these reaction forces tend to decrease if the sliding displacement is extended over 1.5 mm, where it might be close to periodic forces.

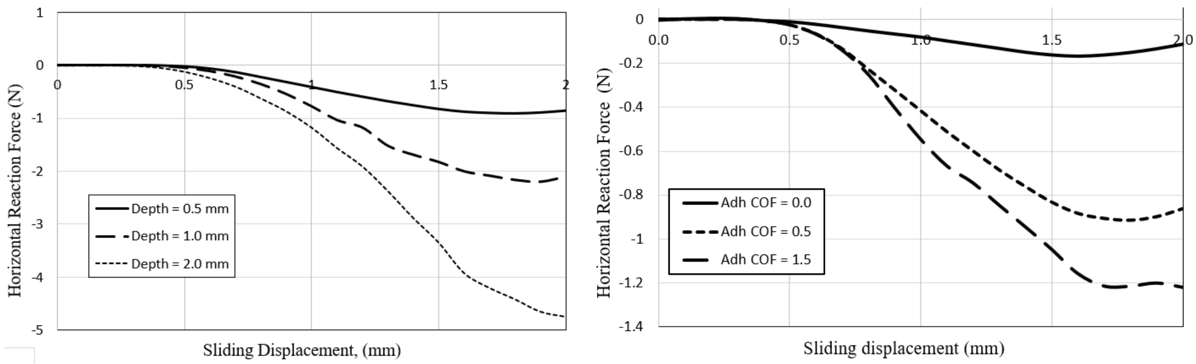

(a) (b)

Figure 5. Horizontal reaction force (a) by various sliding depth for adhesion COF = 0.5 and (b) by various adhesion COF for sliding depth 0.5 mm

The vertical reaction forces have relative constant value for low value of the adhesion COF and sliding depth, meanwhile, fluctuative values are obtained for the high value of the sliding depth as well as the adhesion COF. For high adhesion COF, it indicates any oscillation force that may also indicates any oscillation of the rubber surface along friction. In the contact between indenter tip and rubber surface, high adhesion causes high tangential force, therefore, stick occurrence is emerged in addition to slip occurrence. Thus, the stick-slip occurrence causes periodic or oscillation motion and this will lead to the emergence of oscillation forces. This phenomenon also occurs to the case of large sliding depth, that it causes high normal force, therefore, the tangential force is also high and the stick-slip occurrence is also emerged [14].

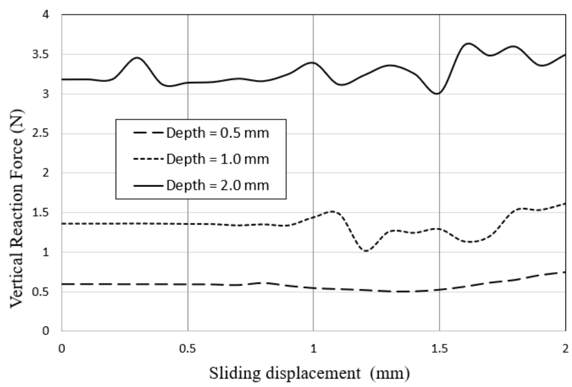

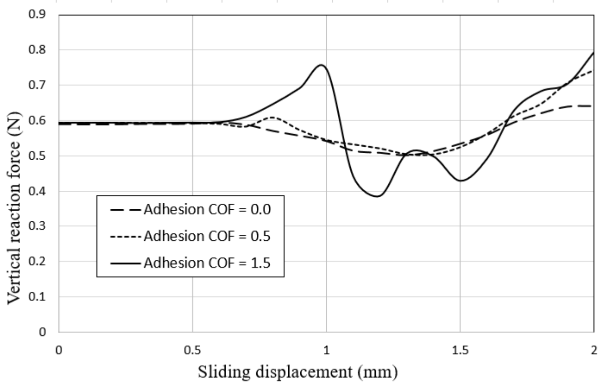

(a) (b)

Figure 6. Vertical reaction forces (a) by various sliding depth for adhesion COF = 0.5 and (b) by various adhesion COF for sliding depth 0.5 mm

Finally, the overall COF can be found by dividing the horizontal reaction forces with the vertical reaction forces. These results are depicted in Fig. 7 that is presented with respect to the sliding displacement.

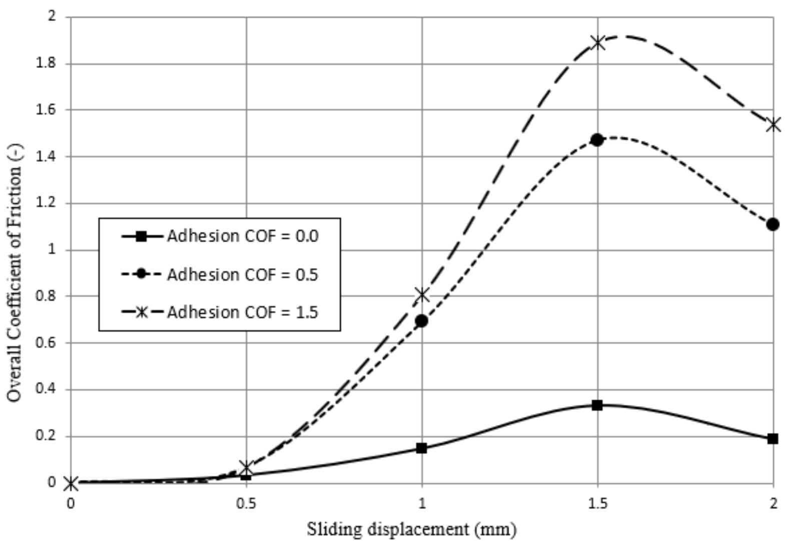

Figure 7. The overall coefficient of friction by given various adhesion COF for sliding depth 0.5 mm

Based on Fig.7, the overal COF highly increases and then decreases with respect to the sliding displacement. This overall COF tends to oscillatory change that might indicate the stick-slip occurrence along friction contact. These phenomena qualitatively are in accordance with the experimental results that the periodic value of COF occured along friction contact [6,15]. By the given constant adhesion COF, the overall COF is strongly influenced by the deformation COF component. In general, it indicates that the overall COF is dominantly influenced by the deformation component rather than the adhesion [11]. The deformation COF is developed from the friction force due to a tangential elastic force in the stick-slip contact. The deformation COF has fluctuative or periodic value that might follow the stick-slip theory. Theoretically, most of the stick-slip analysis is based on the static friction to represent a stick phase and kinetic friction to represent a slip phase [14].

IOP Conf. Series: Journal of Physics: Conf. Series **1090** (2018) 012078 doi:10.1088/1742-6596/1090/1/012078

4. Conclusion

This paper proposes a numerical investigation to identify the friction contact on the rigid blade sliding along unfilled rubber surface. Because of its hyperelastic behaviour, the elastic force has a dominant contribution on the friction force. And also, nonlinear behaviour of the rubber makes the sliding system difficult to be analitically investigated. Coefficient of friction (COF) is the main parameter of the friction contact that commonly consists of adhesion and deformation components. With the given constant adhesion COF, the deformation COF is strongly influenced by the sliding displacement and sliding depth. With the given adhesion COF, the overall COF highly increase and then decreases with respect to the sliding displacement. In general, the overall COF is dominantly influenced by the deformation component than the adhesion one. Qualitatively, the deformation COF tends to follow the stick-slip theory.

References

[1] MSC Software Whitepaper 2010 *Nonlinear Finite Element Analysis of Elastomer* (Santa Ana, USA: MSC Software Corporation)
[2] Johnson K L 1985 *Contact Mechanics* (Cambridge, UK: Cambridge University Press)
[3] Lafaye S 2008 *Wear* **264** 550-554
[4] Pinnington R J 2009 *Wear* **267** 1653–1664
[5] Vieira T, Ferreira R P, Kuchiishi A K, Bernucci L L B and Sinatora A 2015 *Wear* **328-329** 556–562
[6] Mane A, Loubet J L and Guerret C 2013 *Wear* **306** 149–160
[7] Coveney V and Menger C *Wear* **233-235** 702-711
[8] Zhang S W 2004 *Tribology of Elastomer, Tribology and Interface Engineering Series* (Amsterdam: Elsevier)
[9] Uchiyama Y and Ishino Y 1992 *Wear* **158** 141-155
[10] Liang H, Fukahori Y, Thomas A G and Busfield J J C 2009 *Wear* **266** 288-296.
[11] Wu Y P, Zhou Y, Li J L, Zhou H D, Chen J M and Zhao H C 2016 *Wear* **356-357** 1–8
[12] Liang H 2007 *Investigating the Mechanism of Elastomer Abrasion* (London, UK: PhD Thesis, University of London)
[13] ABAQUS 6.11 2011 *Standard User's Manual* (USA: Dassault Systems Simulia Corp.)
[14] Setiyana B, Ismail R, Jamari J and Schipper D J 2016 *Tribol. Online* **11,3** 512-518
[15] Rorrer R and Eiss N S 1995 *Tribol. Transaction* **38,2** 323-328